Advanced Journal of Chemistry-Section A, 2020, 3(3), 289–300
Available online at : www.ajchem-a.com
ISSN Online: 2645-5676
DOI: 10.33945/SAMI/AJCA.2020.3.7

Original Research Article

Effective Removal of Cd(II) and Pb(II) from Aqueous Solution by Synthesized Palladium Nanoparticles Using Spent $PdCl_2$ Catalyst: Experimental Design and Optimization

Ozra Alimohammadi*

Department of Chemistry, Islamic Azad University, Saveh Branch, Iran

ARTICLE INFO

Received: 08 July 2019
Revised: 07 August 2019
Accepted: 07 September 2019
Available online: 16 September 2019

KEYWORDS

Palladium nanoparticles
Adsorption
Heavy metal ions removal
Recycling
Experimental design

ABSTRACT

Environmental considerations have motivated the present study to develop and to investigate Cd(II) and Pb(II) removal process from aqueous solutions. This was carried out through the application of ultrasound onto sodium dodecyl sulfate coated palladium nanoparticles (SDSPdNPs). The recovered palladium chloride of petroleum's spent catalyst used as a precursor for the nanoparticle synthesis. The size, morphology and the structure of the synthesized adsorbent has been fully characterized using transmission electronic microscope (TEM), scanning electron microscope (SEM), and X-ray diffractometer (XRD) spectroscopy measurements. The mean diameter of the SDSPdNPs as typically 23.4 nm for a generally homogeneous size regardless of agglomeration is reported. Statistically designed experiments with the support of central composite design (CCP) and response surface methodology (RSM) were applied to evaluate the main physiochemical parameters that would affect the interactions among the variables with the aim to define optimization criteria for the adsorption efficiency with respect to both of the metal ions. The optimized condition is reported as follows: pH: 4.2; contact time: 92 min; adsorbent dosage: 65 mg. Further to the above findings, the experimental equilibrium data efficiency fitted the Langmuir model with a high adsorption capacity of 323.14 and 207.81 mg/g^{-1} in the case of Pb(II) and Cd(II), respectively.

GRAPHICAL ABSTRACT

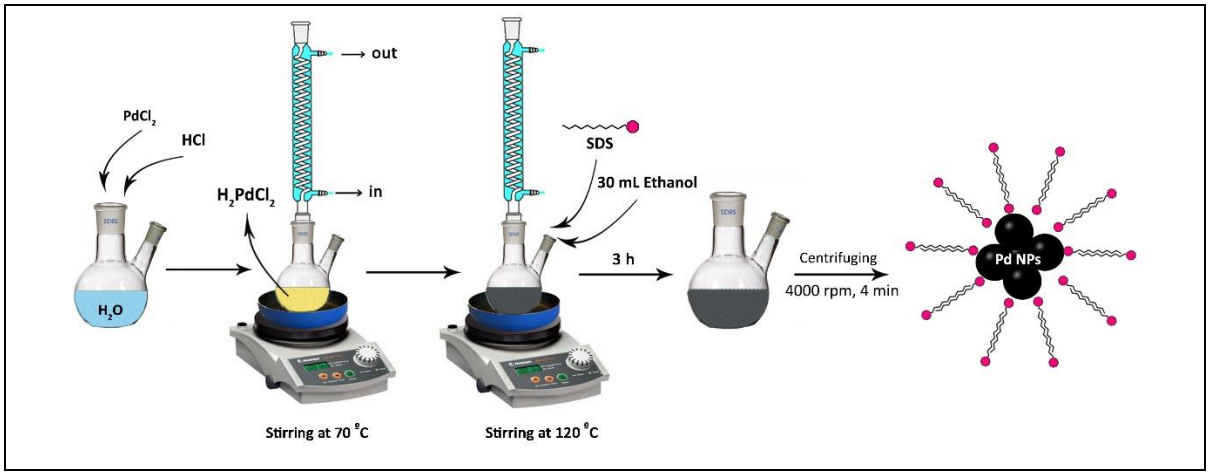

* Corresponding author's E-mail address: Lalimohammadi60@gmail.com

Introduction

The current century faces the worldwide environmental problem of heavy metal contamination. Unlike most organic contaminants, these metals are not biodegradable in the environment and they are toxic as well [1,2]. The tendency to accumulate in living organisms is high among them and this might result in severe harms and incurable health problems to animals, plants, and human beings via food chain transfers [3,4]. The rapid industrial growth has led to direct and indirect discharging of contaminated wastewaters with toxic heavy metals into the environment [5-7]. Cadmium and lead are considered as the most dangerous pollutant elements [8]. Up to now, different kinds of physical and chemical methods like ion exchange [9], adsorption [10-13], chemical precipitation [14], reverse osmosis [15] and membrane process [16] have been used to separate heavy metal ions from wastewater. Among the existing methods, adsorption technology is the most favorable and frequently used technique because of its low cost, simplicity, and high efficiency [17,18]. Newly, many investigation groups have studied several nanoparticles for removal goals. Increased surface reactivity, unusual adsorption capacity, modified electrochemical potentials, new catalytic properties, feasibility of versatile functionalization, and so on, are all the features used in this regard [19].

Palladium nanoparticles (PdNPs) and its nanocomposites have been successfully used for removal of some hazard materials from various samples by either adsorption or catalytic removal mechanisms. PdNPs loaded on activated carbon have been used for efficient removal of some dyes such as methylene blue [20], congo red [21], and bromophenol red [22] and also palladium-modified nitrogen-doped titanium oxide has been used for removal of As (III) [23].

Response surface methodology (RSM) is a set of mathematical and statistical approaches used for designing, improving and optimizing processes [8-24]. This method can be utilized for evaluating the effects of individual parameters, their relative significance and the interaction of two or more variables and determining the optimum conditions for desired responses [24,25]. The main objective of RSM is to determine the optimum operating conditions for the system or to determine a region that satisfies the operating specifications [26]. The RSM approach usually includes the following two steps: the first step is the model formulation to determine which factors and their interactions significantly affect the response, and the second step is the optimization of the factors that influence the performance of the response [27].

In the current study, we represent our preparation and characterization of sodium dodecyl sulfate coated palladium nanoparticles (SDSPdNPs) as an adsorbent for efficient removal of Pb(II) and Cd(II) from water samples. The SDSPdNPs have been synthesized from recovered palladium chloride of olefin unit of the Iran-Arak-Shazand petroleum's spent catalyst. The impacts of some physicochemical parameters, i.e. pH, sonication time and adsorbent dosage on the adsorption efficiency of the studied heavy metal ions on SDSPdNPs were explored. A central composite design (CCD) combined with RSM were used to do statistically designed experiments in order to determine variables which have effect on the heavy metal removal efficiency in significant way.

Experimental

Materials and Methods

Reagents and apparatus

Recovered palladium chloride ($PdCl_2$) of olefin unit of the Iran Arak Shazand petroleum spent catalyst was used as appropriate

precursor for the nanoparticles synthesis. All of the other chemicals used were of analytical reagent grade and were purchased from Merck Company (Darmstadt, Germany). Aqueous solutions of chemicals were prepared with double distilled water (DDW). The glass equipment's kept in HNO_3 solution overnight and washed with DDW water several times; oven dried and kept in closed bags before use. Stock solutions of Pb(II) and Cd(II) ions were prepared from the nitrates of these elements each as 1000 $mg_/L^{-1}$. Working solutions, as per the experimental requirements, were freshly prepared from the stock solution for each experimental run. The adjustments of pH were performed with 0.01-1.0 mol/L^{-1} HCl and/or NaOH solutions.

The concentration of the metal ions was determined by atomic absorption spectrometry (AAS), (Spect AI 1200, Aurora, Canada). The instrumental settings of the manufacturer were followed. The size, morphology and the structure of the synthesized nanoparticles were characterized by a transmission electronic microscope (TEM), (EM 208-100 KV-Philips, Netherlands) and a scanning electron microscope (SEM), (VEGA II, TESCAN, and Czech). The crystal structure of the synthesized materials was determined by an X-ray diffractometer (XRD), (38066 Riva, d/G. via M. Misone, 11/D (TN), Italy) at ambient temperature. A pH-meter (Metrohm model 713, Herisau, Switzerland) with a combined glass electrode was used for pH measurements. An ultrasonic cleaner water bath (40 kHz universal, RoHS, Korea) was used. Infrared spectra's of the adsorbent and SDS collected using a FT-IR spectrometer (Perkin-Elmer model Spectrum GX) with the spectral range of 4000–400 cm^{-1}.

Preparation of sodium dodecyl sulfate coated palladium nanoparticles (SDSPdNPs)

Typically, 0.178 g of $PdCl_2$, 2.0 mL of 2.0 M HCl and 500 ml of DDW water were mixed to get H_2PdCl_4 solution. Then, the total volume was put in a flask, refluxed and allowed the reaction to proceed completion. The color of the product was typically pale-yellow. Then, 30 mL of the solution was mixed with 2.0 g sodium dodecyl sulfate (SDS) in 40.0 mL DDW water. Then, the mixture was heated (120 °C) prior to treatment with ethanol (30.0 mL) under reflux for 3 hr to ensure the complete reduction of H_2PdCl_4 and formation of black SDSPdNPs (Figure 1). The product was separated by centrifuging (4000 r/min) and washed with acetone and then ethanol to remove unreacted reagents.

Ultrasound-assisted adsorption method

The metal ions removal was examined using ultrasound power combined with SDSPdNPs.

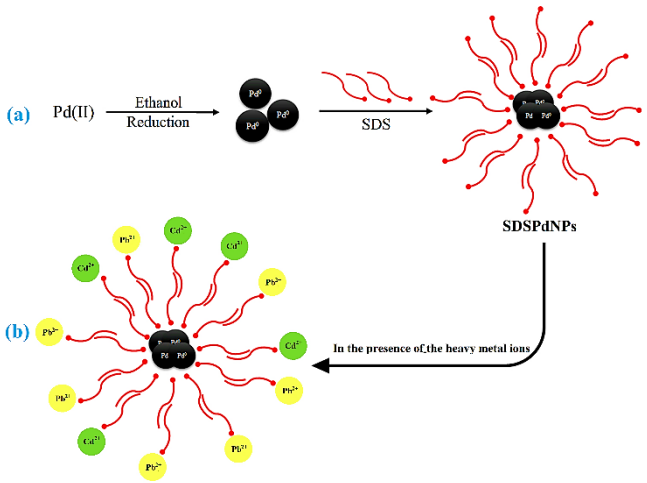

Figure 1. Schematic presentation of (a) overall route for synthesis of SDSPdNPs and (b) the possible the heavy metal ions removal mechanism

The sonochemical adsorption experiment was carried out in a batch mode as follows: specified amounts of the metal ions solution at a known concentration (25 mg/L^{-1}) and initial pH of 4.2 with a known amount of adsorbent (65 mg) were poured into the flask and maintained the desired sonication time (90.0 min) at room temperature (298 K). At the end of the adsorption experiments, the sample was immediately centrifuged and analyzed.

Measurements of the metal ions uptake

The efficiency of the metal ions removal was determined in different experimental conditions designed according to the CCD method. The percent adsorption, i.e., the metal ions removal efficiency (%Re), was determined using the following equation:

$$\%\mathrm{Re} = \left[\frac{C_0 - C_t}{C_0}\right] \times 100\% \quad (1)$$

Where C_0 and C_t represent the initial and final (after adsorption) concentrations of the metal ions in mg/L^{-1}, respectively. Also, all the experiments were performed at room temperature. The adsorbed the metal ions amount (q_e (mg/g^{-1})) was calculated by the following mass balance relationship:

$$q_e = \frac{(C_0 - C_e) \times V}{W} \quad (2)$$

Where C_0 and C_e (mg/L^{-1}) are the initial and equilibrium the metal ions concentrations in aqueous solution, respectively, V (L), the volume of the solution and W (g), the mass of the adsorbent.

Adsorption isotherms

The equilibrium data were analyzed in accordance with the Langmuir and Freundlich isotherm models. The linear form of the Langmuir isotherm is [28]:

$$\frac{C_e}{q_e} = \frac{1}{K_L q_m} + \frac{1}{q_m} C_e \quad (3)$$

Where K_L is a constant and C_e is the equilibrium concentration (mg/L^{-1}), q_e is the amount of solute adsorbed per gram of adsorbent (mg/g^{-1}) at equilibrium concentration C_e, and q_m is the maximum amount of solute adsorbed per gram of surface (mg/g^{-1}), which depends on the number of adsorption sites. The Langmuir isotherm shows that the amount of solute adsorption increases as the concentration increases up to a saturation point. The linear form of Freundlich empirical model is represented by [29]:

$$\ln q_e = \ln k_f + \frac{1}{n} C_e \quad (4)$$

Where K_f ($mg^{1-1/n}$ $L^{1/n}$ g^{-1}) and 1/n are Freundlich constants that depend on temperature and the given adsorbent-adsorbate couple. The parameter n is related to the adsorption energy distribution, and K_f indicates the adsorption capacity.

Central composite design (CCD)

The CCD was used to investigate the significance of the effects of parameters including sonication time, pH and the amount of adsorbent that was designed using Essential Regression Quick Start Guide. A three-level CCD was performed to evaluate the influence of the quantities of removal yield (Table 1) leading to 18 runs for the optimization process. This table shows the experimental design points. The center points are used to determine the experimental error and the reproducibility of the data. The independent variables are coded based on (−1, +1) interval where the low and high levels are coded as −1 and +1, respectively.

Response surface methodology (RSM) role, following the conduction of optimization section and performing distinct experiments

allows for the determination and evaluation of the relative significance of parameters on the process even in systems with complex interactions.

Table 1. Experimental factors and data statistics of model variables in the CCD

Factors			Levels		
			Low (-1)	Central (0)	High (+1)
pH			2.0	4.0	6.0
Sonication time (min)			20.0	70.0	120.0
Adsorbent dosage (mg)			10	50	90
Run	pH	Sonication time (min)	Adsorbent dosage (mg)	Metal ions removal efficiency (%)	
				Pb(II)	Cd(II)
1	3	100	70	88	68
2	3	100	30	88	53
3	5	40	70	88	65
4*	4	70	50	96	79
5	2	70	50	74	59
6*	4	70	50	96	79
7	5	100	70	90	88
8	5	100	30	90	73
9	5	40	30	88	50
10	3	40	30	86	30
11	4	120	50	96	82
12	4	20	50	86	60
13	3	40	70	86	45
14	4	70	90	96	85
15	6	70	50	70	79
16*	4	70	50	96	79
17*	4	70	50	96	79
18	4	70	10	86	53

* Central point

The modeling is performed to estimate the first or second-order polynomial equations, to follow the analysis of variances (ANOVA) that are plotted in a tridimensional graph and to allow for a surface response that corresponds to a response function that is always used for the prediction of real optimum points.

Point of zero charge of the adsorbent (pH_{PZC})

The pH_{PZC} of the SDSPdNPs was determined in degassed 0.01 mol/L^{-1} $NaNO_3$ solution at 20 °C. Aliquots of 30 mL 0.01 mol/L^{-1} $NaNO_3$ were mixed with 30 mg SDSPdNPs in several beakers. The pH of the solutions was adjusted at 2.0, 3.0, 4.0, 5.0, 6.0, 7.0, 8.0 and 9.0 using 0.01 mol/L^{-1} of HNO_3 and/or NaOH solutions as appropriate. The initial pHs of the solutions were recorded, and the beakers were covered with parafilm and shaken for 24 h. The final pH values were recorded and the differences between the initial and the final pH (the so-called ΔpH) of the solutions were plotted against their initial pH values. The pH_{PZC} corresponds to the pH where ΔpH=0 [30]. The pH_{PZC} for SDSPdNPs was determined using the above procedure and was obtained as almost 3.0 (Figure 2).

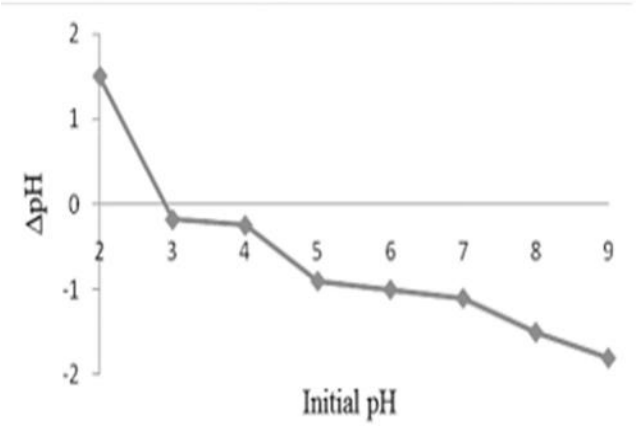

Figure 2. Point of zero charge (pHpzc) of SDSPdNPs

Results and discussion

Characterization of the adsorbents

The XRD pattern of the synthesized SDSPdNPs (Figure 3) shows diffraction peaks that are indexed to (1 1 1), (2 0 0), (2 2 0), (3 1 1) and (2 2 2) reflection characteristics of the face centered cubic phase of the metallic palladium [31]. The crystallite size of palladium nanoparticle was calculated using Sherrer's formula,

$$d = 0.94\,\lambda\,/\beta\cos\theta$$

Where, λ is wavelength and β is full width half maximum of corresponding peak. A peak position at 2θ was used for calculating the crystalline size and the size of the PdNPs was calculated as 12 nm, which supports the TEM results.

SEM image of the synthesized nanoparticles has been depicted in Figure 4a. From this Figure it can be concluded that almost uniform spherical monodisperse nanoparticles with average diameter of 58.6 nm have been synthesized. TEM (Figure 4b) revealed the diameters of the SDSPdNPs as typically 23.4 nm for a generally homogeneous size. As the results show, the particle dimension obtained by SEM is higher than the corresponding TEM size and/or than the corresponding crystallite size. This difference may be explained due to the presence of aggregates in SEM grain consisting of several crystallites and/or poor crystallinity.

The FT-IR spectra of SDS and SDSPdNPs are presented in Figure 5a and 5b respectively. New absorption peak at almost 1250 cm^{-1} was observed in Figure 5b, that was attributed to S=O groups of SDS (in accordance with Figure 5a) in final product. Moreover, new absorption peaks at almost 2919 and 2851 cm^{-1} are assigned to stretching mode of the aliphatic C-H groups of SDS (In accordance with Figure 5a). Based on the above results, it can be concluded that the fabrication procedure has been successfully performed.

Central composite design (CCD)

The CCD step (Tables 1) was used to estimate the main interaction of variables: pH (X_1), sonication time (X_2) and adsorbent dosage (X_3) through 18 experiments in three levels (low, basal and high) with the coded values of (−1, 0, +1) respectively. Generally, in such optimization, the protocol application of the analysis of variances (ANOVA) (Table 2) helps the researchers to evaluate the most significant variables and their interaction based on *F*-test and considering p-value at 95% confidence level.

Figure 2. XRD patterns of the SDSPdNPs

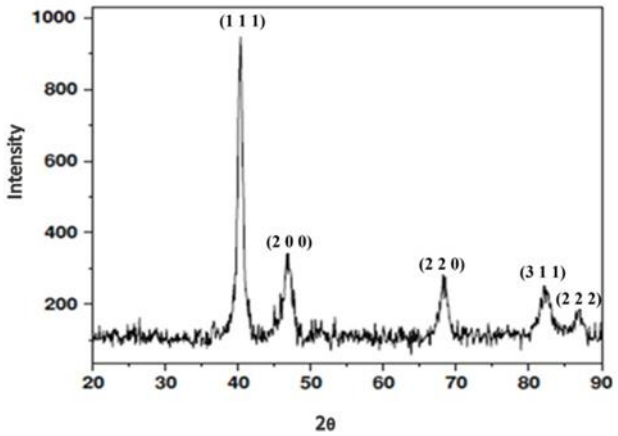

Figure 3. (a) SEM and (b) TEM image of the SDSPdNPs

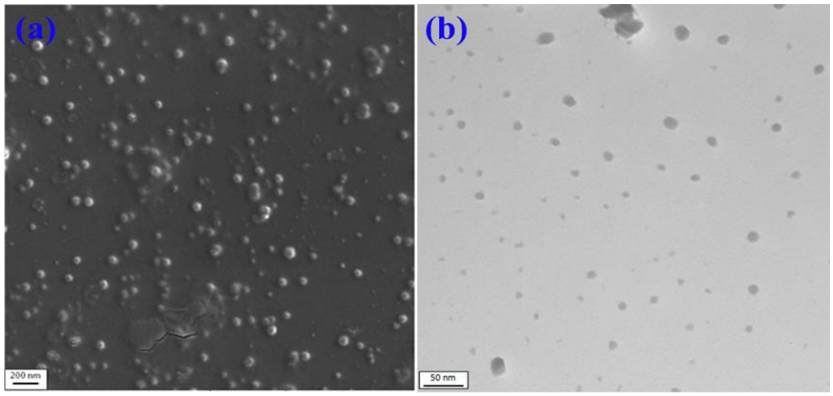

Figure 4. FT-IR spectra of (a) SDS and (b) SDSPdNPs

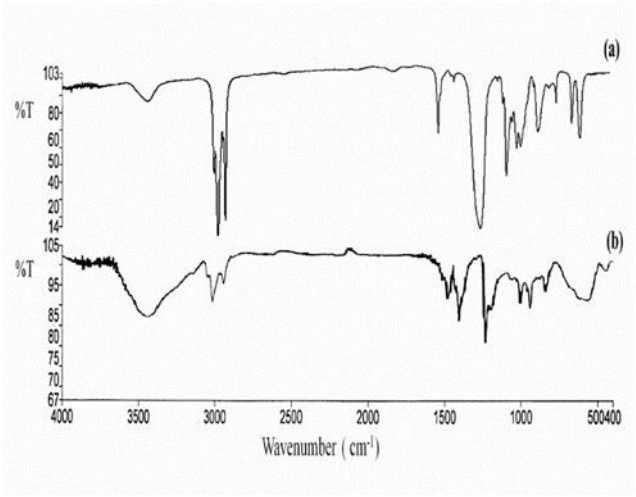

Data analysis gave a semi-empirical expression of removal efficiency (Y) in Eqs. (5 and 6) as follow:

$$Y_{Pb} = -21.64 + 47.27X_1 + 0.308X_2 + 0.352X_3 - 5.908X_1^2 + 2.0123E\text{-}14\ X_1 X_2 - 1.27112E\text{-}15\ X_1 X_3 - 0.00176\ X_2^2 + 5.30154E\text{-}17\ X_2 X_3 - 0.0029\ X_3^2 \quad (5)$$

$$Y_{Cd} = -107.69 + 37.56\ X_1 + 1.192\ X_2 + 1.327\ X_3 - 3.757\ X_1^2 + 3.03E\text{-}16\ X_1 X_2 - 2.69304E\text{-}17\ X_1 X_3 - 0.00626\ X_2^2 + 7.62768E\text{-}18\ X_2 X_3 - 0.00939\ X_3^2 \quad (6)$$

Response surface methodology

RSM application following CCD helps the investigators to optimize the significant factors and to provide valuable information about response nature. Figure 6 shows the

relevant fitted response surfaces for the design and represents the response surface plots of %Re versus variables, whereas their curvatures depict the existence of interaction among variables.

The response surface plots (Figure 6A (a–c) and 6B (a-c)) illustrate the dependency of removal percentage on variables such as adsorbent dosage, contact time and pH. The removal percentage has a similar and positive trend with adsorbent dosage and higher removal percentage at higher adsorbent mass is attributed to its higher specific surface area. With lower amounts of adsorbent, a significant decrease in the removal percentage was observed because of the possible saturation of reaction sites.

Figure 6A (c and b) and 6B (c and b) presents the interaction of pH with mass of adsorbent and sonication time, respectively. The adsorption amounts increased and then decreased when the pH increased. The observed dependency of removal percentage on pH maybe attributed to change in the surface of the adsorbents with change in pH, which was consistent with the pH-dependent zeta-potential of SDSPdNPs. The pH of zero-point charge (pH_{pzc}) was 3.0. At low pH (pH <pH_{pzc}), the surface of the adsorbents presents in positive (or neutral) form and has less adsorption. As the alkalinity of solution increases, the surface of the adsorbents presents in negative and electrostatic attraction forces between the cations and negatively charged adsorbent is responsible for high removal percentages.

Figure 6A (a and b) and 6B (a and b) confirms that maximum the metal ions adsorption could occur at a sonication time of above 93 and 87 min for Cd(II) and Pb(II), respectively, showing the rapidity and high efficiency of the adsorbent. The initial fast adsorption is attributed to the increase in available surface area and vacant site following the efficient dispersion of adsorbent into the solution by ultrasonic power. It was found that more than 88% and 96% of Cd(II) and Pb(II) removal occurred in the first 93 and 87 min, respectively. The almost high rapidity of adsorption process is related to the fact that ultrasonic irradiations simultaneously increase the diffusion coefficient of the metal ions and the surface reactive atoms and the area of adsorbent. The optimum conditions for the metal ions removal by SDSPdNPs including adsorbent dosage, contact time, and pH were obtained 65 (mg), 92 (min), 4.2 respectively. Metal ions removal efficiency for Cd(II) was 84% and for Pb(II) was 95%. The plot of the experimental values of removal (%) values versus those calculated from the equation, indicated a good fit.

Table 2. Analysis of variance (ANOVA) for CCD

Source of variation	Pb(II)				Cd(II)			
	Sum of square	Degree of freedom	Mean square	F-value	Sum of square	Degree of Freedom	Mean square	F-value
Regression	861.60	6	143.60	27.05	3711.0	9	412.33	4.298
Residual	58.40	11	5.309		767.54	8	95.94	
Lack of Fit	-	-	-	-	760.79	5	152.16	67.6257
Pure error	-	-	-		6.750	3	2.250	
Total error	920.00	17			4478.5	17		

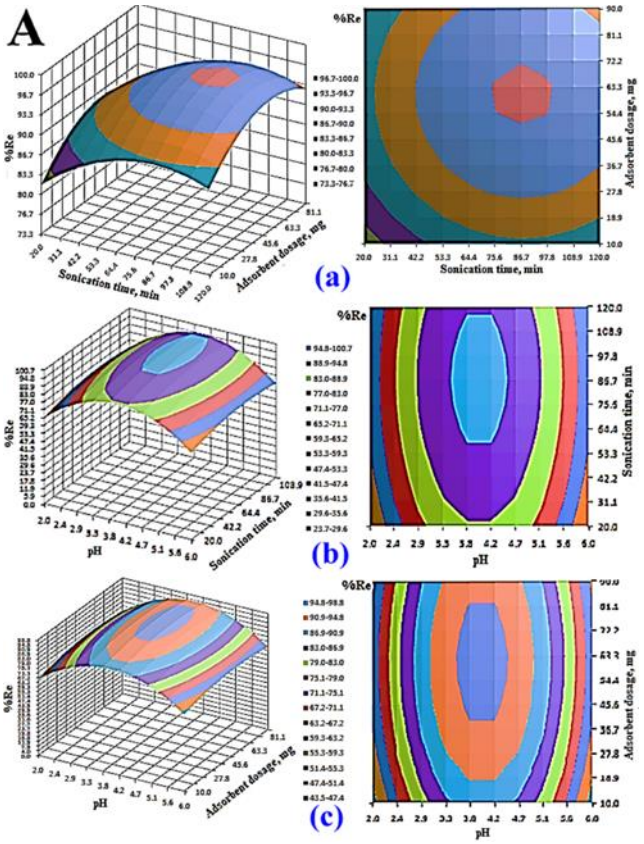

Figure 5. Response surfaces for the CCD of (A) Pb(II) and (B) Cd(II) ((a) adsorbent dosage-sonication time (b) pH-sonication time and (c) pH-adsorbent dosage)

Adsorption isotherms and adsorption mechanism

The equilibrium data were analyzed in accordance with the Langmuir and Freundlich isotherm models. After the equilibrium adsorption data (Figure 7) were fitted with the isotherm models using nonlinear regression, the fitting parameter values are summarized in Table 3.

The higher correlation coefficient obtained for the Langmuir model indicates that the experimental data are better fitted into this model, and adsorption of the metal ions on SDSPdNPs adsorbents is more compatible with Langmuir assumptions, *i.e.,* adsorption takes place at specific homogeneous sites within the adsorbent. The Langmuir model is based on the physical hypothesis that the maximum adsorption capacity consists of a monolayer adsorption, that there are no interactions between adsorbed molecules, and that the adsorption energy is distributed homogeneously over the entire coverage surface. A possible mechanism for monolayer adsorption of the analytes is the electrostatic attraction forces between the metal cations and the anionic surfactant [32] (SDS) as schematically depicted in Figure 1b. The Langmuir sorption model serves to estimate the maximum uptake values where they cannot be reached in the experiments. According to the results (Table 3), the adsorption capacities for the adsorption of Pb(II), and Cd(II) by the SDSPdNPs, expressed by Langmuir coefficient qm, demonstrate that adsorption capacity increased in the sequence of Pb(II)>Cd(II), where the different adsorption capacity maybe is due to disparity in cations radius and interaction enthalpy values.

Desorption and repeated usage

From practical perspective, repeated availability is a crucial attribute of an advanced adsorbent. For desorption research, firstly metal adsorbed SDSPdNPs were washed by ultrapure water to remove the un-adsorbed

metals that loosely attached to the vial and adsorbent.

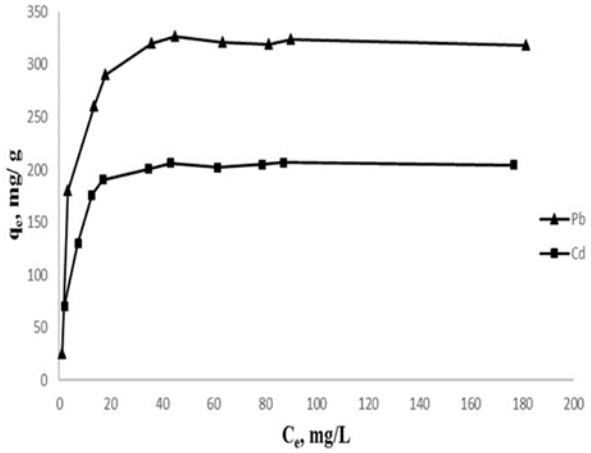

Figure 6. Isothermal adsorption curve of (▲) Pb(II) and (■) Cd(II) on SDSPdNPs

Table 3. Adsorption isotherm parameters for the adsorption isotherm models for the adsorption of investigated cations onto SDSPdNPs at 298 K

Isotherm models	Parameters	Metal ions	
		Pb(II)	Cd(II)
Langmuir	K_L(L/g^{-1})	13.25	5.71
	q_m(mg/g^{-1})	332.9	210.5
	r^2	0.986	0.978
Freundlich	K_f(mg$^{1-1/n}$ L$^{1/n}$ g^{-1})	42.3	28.4
	1/n	0.176	0.388
	r^2	0.816	0.789

For the purpose of estimating the recovery of the metal ions from the adsorbent, desorption experiments with various reagents (0.1 M HCl, 0.1 M HNO3 and mixture of acetonitrile: 0.1 M HNO3 (1:1 v/v)) were conducted. The adsorbent was separated after adsorption of the metal ions. Afterwards 4.0 mL of the eluents was added to the separated adsorbent. Samples were collected after 5, 10, 20 and 30 min contact times with the eluent in order to evaluate metal recovery by an atomic absorption spectrophotometer. Findings showed that mixture of acetonitrile with 0.1 M HNO_3 is effective as a back-extractant and can be employed for the quantitative recovery of the metal ions. It was found that desorption rate was very rapid since almost 97% desorption completed within 20–25 min for both of the metal ions. Likewise, the metal ion adsorption capacity of the adsorbent remained almost constant for the 10 cycles, which shows no irreversible sites on the surface of SDSPdNPs for desorption with mixture of acetonitrile with 0.1 M HNO_3 and the reusability of the adsorbents was satisfactory. Our recyclability studies indicate that this nano-adsorbent can be frequently used as an efficient adsorbent in water treatment.

Conclusion

It was observed that SDSPdNPs is an efficient adsorbent for the removal of Cd(II) and Pb(II) cations. In the present research, the analysis of the results by CCD allows for the achievement of the following optimization point: 65 mg of adsorbent, 92 min of contact time and at pH of 4.2. The equilibrium studies

were investigated for the adsorption process. The experimental equilibrium data efficiency fitted the Langmuir model with a high adsorption capacity of 323.14 and 207.81 mg/g^{-1} in the case of Pb(II) and Cd(II), respectively.

Acknowledgement

The authors greatly appreciate Shazand Petrochemical Company for supplying spent palladium chloride catalyst to this research work.

Disclosure statement

No potential conflict of interest was reported by the author.

References

[1] J. Liang, X. Li, Z. Yu, G. Zeng, Y. Luo, L. Jiang, Z. Yang, Y. Qian, H. Wu, *Acs. Sustain. Chem. Eng.*, **2017**, *5*, 5049–5058.

[2] M. Bali, H. Tlili, *Int. J. Environ. Sci. Technol.,* **2019**, *16*, 249–258.

[3] J. Song, H. Kong, J. Jang, *J. Coll. Interface Sci.,* **2011**, *359*, 505–511.

[4] I.M. Kenawy, M.A.H. Hafez, M.A. Ismail, M.A. Hashem, *Int. J. Biol. Macromol*., **2017**, 1538–1539.

[5] S. Guo, P. Jiao, Z. Dan, N. Duan, J. Zhang, G. Chen, W. Gao*, Chem. Eng. Res. Des.,* **2017**, *126*, 217–231.

[6] L.L. Ling, W.J. Liu, S. Zhang, H. Jiang, *Environ. Sci. Technol.,* **2017**, *51*, 10081–10089.

[7] T. Madrakian, A. Afkhami, M. Ahmadi, *Chemosphere,* **2013**, *90*, 542–547.

[8] A. Ahmadi, S. Heidarzadeh, A.R. Mokhtari, E. Darezereshki, H.A. Harouni, *J. Geochem. Explor.,* **2014**, *147*, 151–158.

[9] L. Dong, L.A. Hou, Z. Wang, P. Gu, G. Chen, R. Jiang, *J. Hazard. Mater.,* **2018**, *359*, 76–84.

[10] D. Huang, J. Wu, L. Wang, X. Liu, J. Meng, X. Tang, C. Tang, J. Xu, *Chem. Eng. J.,* **2018**, *358*, 1399–1409.

[11] N. Koukouzas, C. Vasilatos, G. Itskos, I. Mitsis, A. Moutsatsou, *J. Hazard. Mater.,* **2010**, *173*, 581–588.

[12] T. Madrakian, A. Afkhami, B. Zadpour, M. Ahmadi, *J. Ind. Eng. Chem*., **2015**, *21*, 1160–1166.

[13] M.A. Tofighy, T. Mohammadi, J. *Hazard. Mater.,* **2011**, *185*, 140–147.

[14] F. Fu, L. Xie, B. Tang, Q. Wang, S. Jiang, *Chem. Eng. J.,* **2012**, *189-190*, 283–287.

[15] Y. Li, Z. Xu, S. Liu, J. Zhang, X. Yang, *Comput. Mater. Sci.,* **2017**, *139*, 65–74.

[16] L. Zhang, Q. Huang, *Environmental Fate, Transport, and Transformation of Carbon Nanoparticles, Biotechnology and Nanotechnology Risk Assessment*: Minding and Managing the Potential Threats around Us, American Chemical Society, Georgia, **2011**, pp. 69–101.

[17] F. Ge, M.M. Li, H. Ye, B.X. Zhao, *J. Hazard. Mater.,* **2012**, *211-212*, 366–372.

[18] T. Madrakian, A. Afkhami, M. Ahmadi, H. Bagheri, *J. Hazard. Mater.,* **2011**, *196*, 109–114.

[19] T. Pradeep, M.S. Bootharaju, 13-Noble Metal Nanosystems for the Detection and Removal of Pollutants in Drinking Water, in: S. Ahuja (Ed.) *Water Reclamation and Sustainability*, Elsevier, Boston, **2014**, pp. 317–342.

[20] M. Ghaedi, S. Heidarpour, S. Nasiri Kokhdan, R. Sahraie, A. Daneshfar, B. Brazesh, *Powder Technol.,* **2012**, *228*, 18–25.

[21] M. Ghaedi, M.N. Biyareh, S.N. Kokhdan, S. Shamsaldini, R. Sahraei, A. Daneshfar, S. Shahriyar, *Mater. Sci. Eng. C.,* **2012**, *32*, 725–734.

[22] M. Ghaedi, M. Ghayedi, S.N. Kokhdan, R. Sahraei, A. Daneshfar, *J. Ind. Eng. Chem.,* **2013**, *19*, 1209–1217.

[23] S. Poulston, E.J. Granite, H.W. Pennline, H. Hamilton, A.W. Smith, *Fuel*, **2011**, *90*, 3118–3121.

[24] K. Wantala, E. Khongkasem, N. Khlongkarnpanich, S. Sthiannopkao, K.W.

Kim, *Appl. Geochem*., **2012**, *27*, 1027–1034.

[25] S. Demim, N. Drouiche, A. Aouabed, T. Benayad, M. Couderchet, S. Semsari, *J. Ind. Eng. Chem.,* **2014**, *20*, 512–520.

[26] M. Mourabet, E.R. Abdelhadi, H. El Boujaady, M. Bennani-Ziatni, R. El Hamri, T. Abderrahim, *J. Saudi. Chem. Soc.,* **2012**, *19*, 603–615.

[27] F. Absalan, M. Nikazar, *Chem. Eng. Commun.*, **2016**, *203*, 1523–1531.

[28] I. Langmuir*, J. Am. Chem. Soc.,* **1916**, *38*, 2221–2295.

[29] H. Freundlich, W. Heller, J*. Am. Chem. Soc.*, **1939**, *61*, 2228–2230.

[30] T. Madrakian, M. Ahmadi, A. Afkhami, M. Soleimani, *Analyst*, **2013**, *138*, 4542–4549.

[31] D.S. Sheny, D. Philip, J. Mathew, *Spectrochim. Acta A.*, **2012**, *91*, 35–38.

[32] M. Adeli, Y. Yamini, M. Faraji, *Arab. J. Chem.,* **2012**, *10*, 514–521.

How to cite this manuscript: Ozra Alimohammadi, Effective Removal of Cd(II) and Pb(II) from Aqueous Solution by Synthesized Palladium Nanoparticles Using Spent $PdCl_2$ Catalyst: Experimental Design and Optimization*, Adv. J. Chem. A*, **2020**, *3*(3), 289–300.